Supplementary Information

Tyramide Signal Amplification for Highly Sensitive Multiplex Immunoassay based on Encoded Hydrogel Microparticle

Jun Hee Choi,[†a] Young Hee Kim,[†a] Jiwoo Kim,[a] Yong Jun Lim,[a] Min Jung Kim[b] and Ki Wan Bong[*a]

[a] Department of Chemical and Biological Engineering, Korea University, Seoul, 02841, South Korea

[b] Department of Pediatrics, Yongin Severance Hospital, Yonsei University College of Medicine, Yongin-si, 16995, South Korea

† These authors contributed equally to this work

***Correspondence: bong98@korea.ac.kr**

Table of Contents

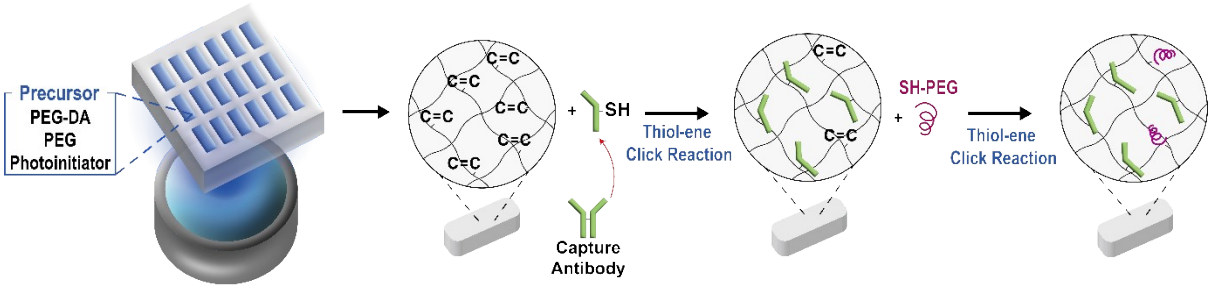

Figure S1. Schematics of hydrogel microparticle synthesis, capture antibody functionalization and elimination of unreacted acrylate double bonds.

Hydrogel microparticles were synthesized using the discontinuous dewetting technique in a degassed micromold. To fabricate the PDMS mold with negative patterns of the encoded microparticles, the PDMS reagents SYLGARD A and B were mixed with a 10:1 volume ratio and poured onto the SU-8 master mold. This mixture was cured for 4 hours in a 70 °C incubator. The patterned PDMS molds were peeled off from the master mold and degassed in a vacuum chamber at 0.1 atm for 15 minutes and then transferred to the glove box at 0% oxygen. The mold was loaded with 10 µL of the precursor, covered with a slide glass and subjected to discontinuous dewetting. The precursor solution was consisted of 75% (v/v) PEG 600, 20% (v/v) PEGDA 700, and 5% (v/v) Darocur 1173. UV exposure time was set to 120 ms, with a regulated UV intensity of 200 mW/cm^2. PBST (1× PBS with 0.05% (v/v) Tween 20) was dropped on the PDMS mold to recover the particles made from photopolymerization. The recovered particle solution was centrifuged at 13,500 rpm for 30 seconds and rinsed three times by substituting 450 µL of the supernatant with PBST.

Following the synthesis, the reduced capture antibodies were immobilized with thiol-ene click reaction to the hydrogel microparticles for target capture. To prevent non-specific bindings, remaining unreacted acrylate groups in the hydrogel particles were eliminated with thiolated polyethylene glycol (SH-PEG), effectively blocking the undesired interactions.

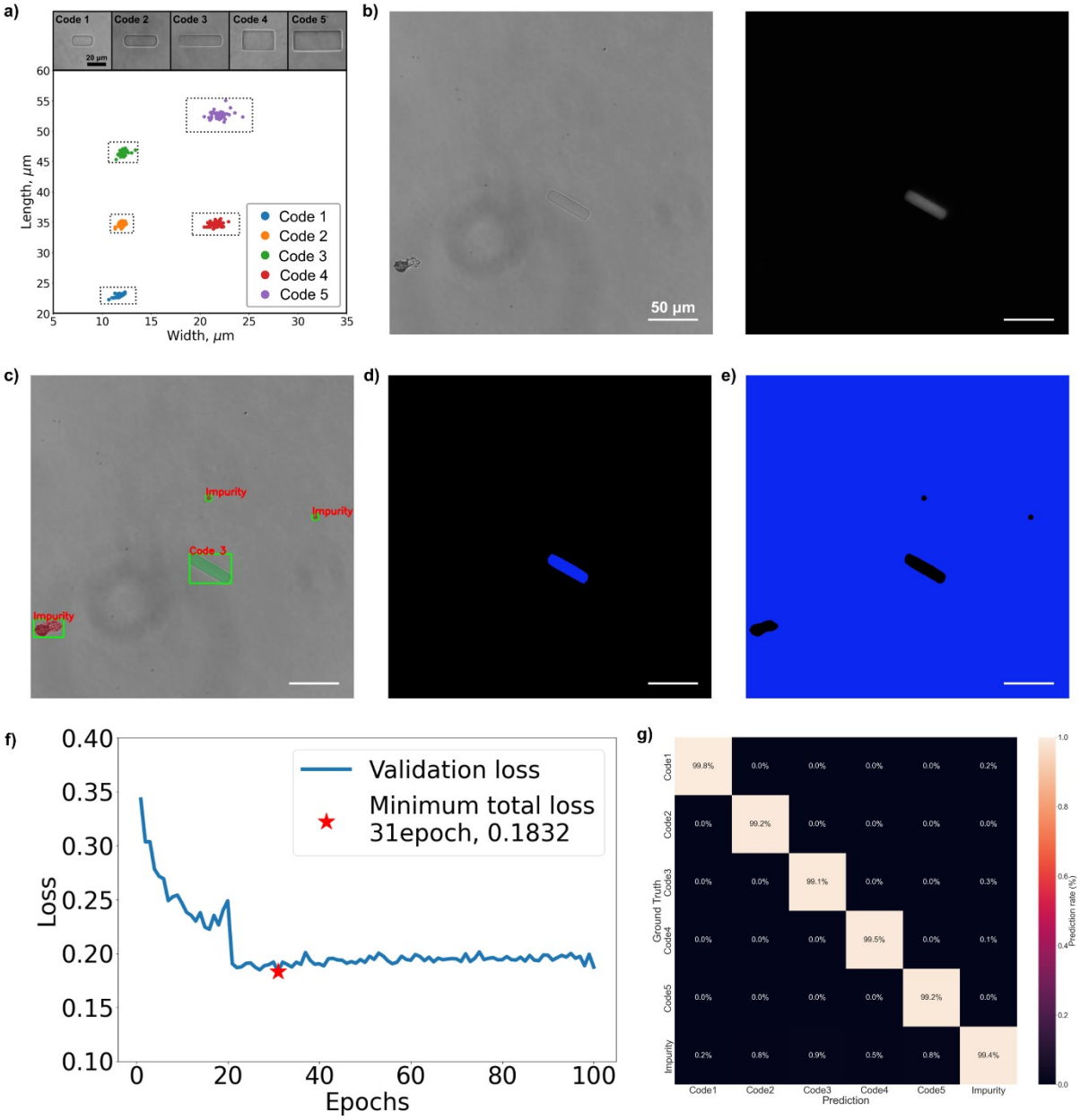

Figure S2. Strategy for graphical encoding and deep learning-based image analysis. (a) The graphically encoded hydrogel microparticles based on the width and length. The dashed boxes indicate the average value ±5× standard deviation of the width and length of each coded particle. (b) A pair of bright-field and fluorescence images used for signal analysis. (c) The bright-field image showing pixel-wise locations of the particles and the impurities by using the deep learning model. (d) A mask used to extract the fluorescence signal from the particle. (e) A mask used to obtain the background signal by excluding the pixels corresponding to the particles or impurities. The blue region indicates the positive location of the mask. (f) The validation loss at each training epoch. (g) Confusion matrix illustrating the accuracy of the deep learning-based decoding software.

Graphical encoding method encodes the information by the shape of the objects. In this study, we utilized the shape of the particles based on the differences in width and length. This method enables the differentiation of the particle information corresponding to the target protein, even when mixed within a single sample. For accurate decoding of the graphically encoded particles, it is crucial to validate that the width and length values measured from the synthesized particles do not overlap. Therefore, the width and length of each coded particle

were measured to confirm this distinction, as shown in Figure S2a. As a result, we verified the absence of overlapping ranges across all types of the coded particles. By this encoding strategy, we functionalized each coded particle with the specific capture antibody: Code1 for IL-4, Code2 for IL-5, Code3 for IL-6, Code4 for IL-9, Code5 for IL-17.

We used the Mask R-CNN model, a well-known deep learning model for instance segmentation, to detect the particles and impurities in the images. This model identifies the pixel-wise locations of the objects and classifies them into categories such as particles or impurities. For the construction of the training data, the objects in each image were labeled as either particles or impurities, using a total of 690 images. These images were divided into training and validation datasets in a 7:3 ratio. During training, we measured the total loss on the validation dataset at each epoch, and the checkpoint that minimized this value was used for assay result analysis.

We used the bright-field images for the input data of the model since the particles with low fluorescence intensities are hard to be detected from the fluorescence image. Thus, we used the bright-field image along with the fluorescence image for analyzing. After getting the mask of each particle, we measured the width and length using the minAreaRect method from the OpenCV library and applied the previously mentioned decoding strategy.

After obtaining the masks for the particles and the impurities, we measured the signal intensity of the particles by calculating the average pixel value within the particle region. Similarly, the background intensity was measured using a background mask generated by inverting the mask containing all particles and impurities. To eliminate inherent background signals, we adjusted the particle intensity by subtracting the background intensity.

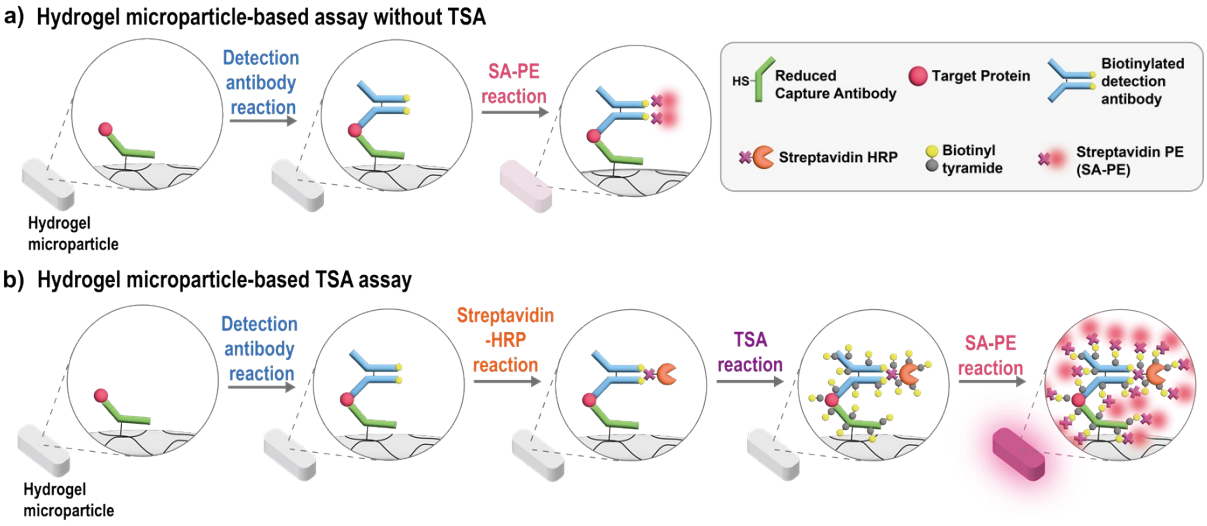

Figure S3. Encoded hydrogel MP-based assay procedures (a) with and (b) without TSA.

The schematic illustrates the encoded hydrogel MP-based assay procedures performed with and without tyramide signal amplification (TSA). The hydrogel MP-based assay without TSA begins with the binding of the target protein to the reduced capture antibody, which is immobilized on the hydrogel MP. This is followed by the introduction of the detection antibody, which binds to another site of the target protein, forming a sandwich complex. The assay concludes with the addition of streptavidin-phycoerythrin (SA-PE), a fluorescence labeling substance that binds to the biotinylated detection antibody. On the other hand, hydrogel MP-based TSA assay adds streptavidin-horseradish peroxidase (SA-HRP) after the introduction of biotinylated detection antibody. Then the TSA reaction is initiated by adding hydrogen peroxide and biotinyl tyramide. The HRP enzyme catalyzes the conversion of tyramide into a reactive radical that covalently attaches to electron-rich residues on the protein, leading to a dense accumulation of biotin molecules. Finally, SA-PE binds to the biotin sites, significantly amplifying the fluorescence signal.

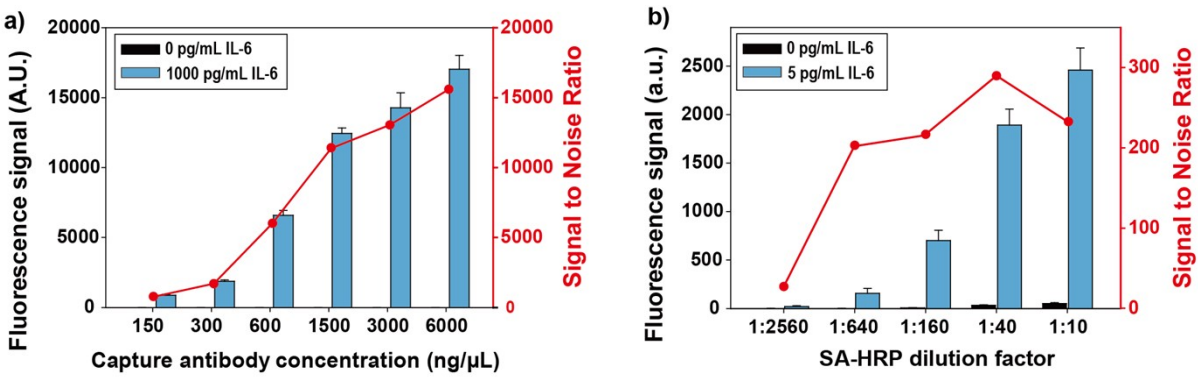

Figure S4. Optimization of (a) capture antibody concentration and (b) HRP dilution factor in the TSA-enhanced hydrogel MP-based immunoassay.

Prior to the application of TSA, we optimized the capture antibody concentration to establish the initial conditions for the immunoassay. The capture antibody concentration was varied from 150 to 6,000 ng/μL, and the fluorescence intensity and signal-to-noise ratio (SNR) were acquired. The results indicate that increasing the capture antibody concentration enhanced the fluorescence signal and the SNR. Therefore, we selected the highest capture antibody concentration as the optimal concentration for each target in subsequent experiments.

For the SA-HRP dilution factor optimization, the hydrogel MP-based TSA assay was utilized. The concentrations of the detection antibody, biotinyl tyramide and TSA reaction time were 0.25 μg/mL, 1 μM and 7 minutes, respectively for all data points. The hydrogel MP used in this process were treated with SH-PEG to minimize the non-specific bindings by blocking the unreacted acrylate groups. Target concentrations of 0 pg/mL and 5 pg/mL IL-6 were detected to acquire the signal-to-noise ratio (SNR). The assay was conducted using different dilution factors of SA-HRP, ranging from 1:2560 to 1:10, to determine the optimal concentration that provides the highest SNR value, while maintaining high fluorescence intensity. As a result, as the dilution factor decreased, indicating higher concentrations of SA-HRP, the SNR increased to reach a peak at a dilution factor of 1:40. Beyond this point, the fluorescence intensity decreased, potentially due to non-specific bindings or saturation. Thus, we determined the optimal dilution factor as 1:40, suggesting that this concentration provides the best balance between the signal intensity and the background noise. This is the same concentration recommended by the manufacturer's protocol for ELISA.

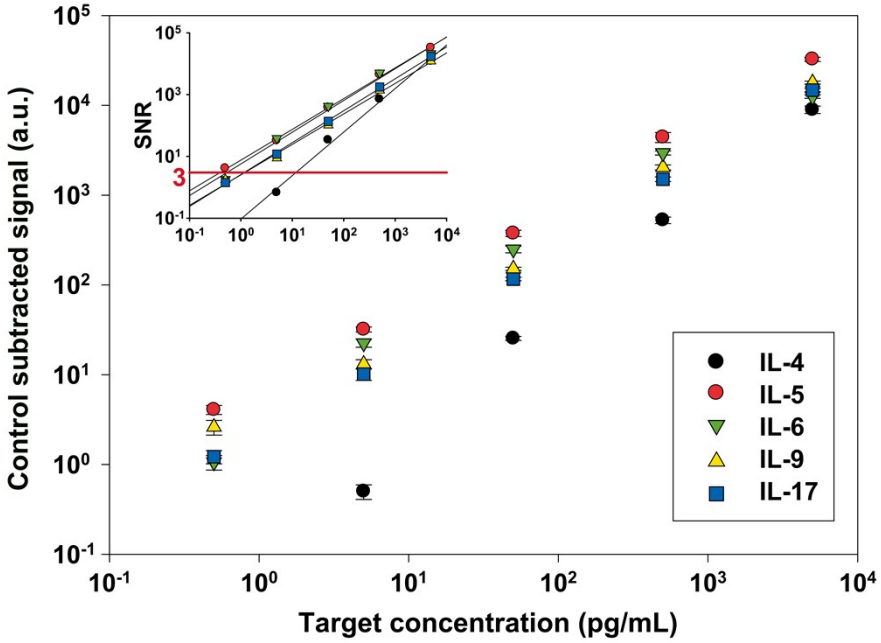

Figure S5. Standard curves and signal-to-noise plots for IL-4, IL-5, IL-6, IL-9, and IL-17 using hydrogel MP-based assay without TSA.

This figure presents the standard curves and signal-to-noise ratio (SNR) plots for IL-4, IL-5, IL-6, IL-9, and IL-17 using conventional hydrogel MP-based assay without TSA. The inset shows the corresponding SNR plots for each target. The red line of the SNR plot is the SNR threshold, which determines the limit of detection (LOD). The assay results suggest that the sensitivity of the hydrogel MP-based assay without TSA is limited for the low target concentrations, emphasizing the potential need of using TSA.

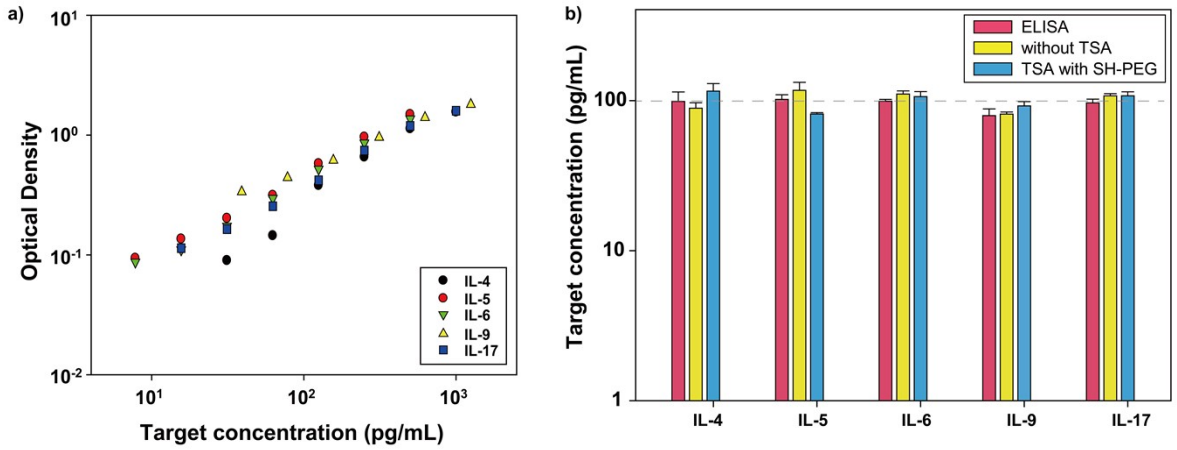

Figure S6. Equivalence test of ELISA, hydrogel MP-based assay without TSA, and hydrogel MP-based TSA assay with SH-PEG. (a) The standard curves for IL-4, IL-5, IL-6, IL-9, and IL-17 using ELISA. (b) The equivalence test between ELISA and hydrogel MP-based assays with and without TSA. The bar graph shows the average of the target concentration and a standard deviation of >7 particles.

To reinforce the reliability of the hydrogel MP-based TSA assay, we conducted an equivalence test comparing the detection results of three different assays: ELISA, hydrogel MP-based assay without TSA, and hydrogel MP-based TSA assay with SH-PEG. We detected IL-4, IL-5, IL-6, IL-9, and IL-17 for this experiment. Each target was spiked-in with a concentration of 100 pg/mL. To calculate the measured target concentrations from the ELISA, we generated the standard curves for the five targets with ELISA according to the manufacturer's user guidelines (Figure S6a). While ELISA experiments were conducted in a singleplex format, the hydrogel MP-based assays with and without TSA were performed in multiplex format. As a result, the measured concentrations match well with the spiked-in concentrations with a deviation of ±20% (Figure S6b), demonstrating the consistency and accuracy among three methods. Consequently, this suggests that hydrogel MP-based assay with and without TSA is a viable alternative to ELISA for multiplex immunoassay.

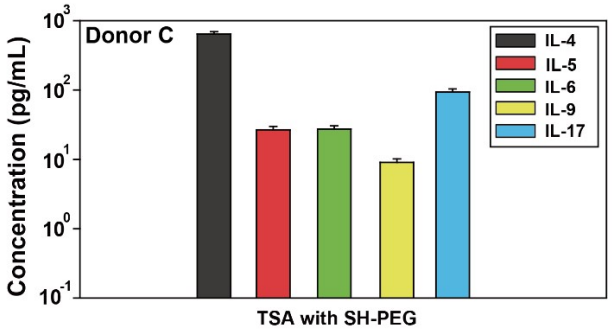

Figure S7. Hydrogel-based TSA assay results for Donor C with an allergic reaction.

Donor C had an allergic reaction due to side effect of Acetaminophen. According to the detection results, Donor C appeared to have elevated levels of IL-4, IL-5, IL-17. This is consistent with the reference that these cytokine concentration increases when allergic reaction occurs.[1, 2]

Table S1. Concentrations of targets and detection antibodies in singleplex assay.

Target protein	*Target concentration (pg/m L)*	*Detection antibody concentration (μg/mL)*
IL-4	**5, 20, 50, 200, 500**	**0.125**
IL-5	**0.1, 0.5, 1, 5, 10**	**0.625**
IL-6	**0.1, 0.5, 1, 5, 50**	**0.25**
IL-9	**0.5, 2, 5, 20, 50**	**1**
IL-17	**0.5, 2, 5, 20, 50**	**0.1**

Table S2. Multiplex detection result of IL-4, IL-5, IL-6, IL-9, and IL-17 using TSA assay with SH-PEG and their recovery.

Case	*Control-Subtracted Signals[a] (a.u.)*				
	IL-4	*IL-5*	*IL-6*	*IL-9*	*IL-17*
1 (- - - - -)	0	0	0	0	0
2 (- + - - -)	(+) 108.5 ± 21.9	136.2 ± 14.7	14.2 ± 1.6	5.9 ± 0.6	24.4 ± 2.2
3 (- + - - -)	0.014 ± 0.0031	(+) 53446.0 ± 6962.1	34.0 ± 3.5	11.0 ± 1.87	74.3 ± 12.4
4 (- - + - -)	9.4 ± 2.6	97.4 ± 11.5	(+) 5202.7 ± 492.9	20.5 ± 4.1	35.5 ± 5.5
5 (- - - + -)	10.4 ± 2.0	19.8 ± 1.7	29.2 ± 3.3	(+) 4893.5 ± 130.3	24.3 ± 2.7
6 (- - - - +)	5.8 ±1.6	37.5 ± 4.1	16.7 ± 2.1	3.0 ± 0.3	(+) 11119.2 ± 1011.6
7 (+ + + + +)	(+) 77.4 ± 3.3	(+) 54611.0 ± 5840.1	(+) 6436.9 ± 1091.2	(+) 4280.4 ± 388.5	(+) 1144.2 ± 87.81
Avg.[b]	93.0 ± 12.6	54028.4 ± 6401.1	5820.0 ± 792.0	4470.0 ± 328.1	11286.7 ± 944.9
Recov.[c] (%)	96.6	98.3	108.0	121.0	123.3

[a] All signals subtracted the control signal (signals of case 1) to exclude the non-specific signals. Each signal is expressed as the mean ± standard deviation of >7 particles. The signs before the signal indicate the presence (+) or absence (−) of the target. IL-4, IL-5, IL-6, IL-9 and IL-17 were spiked at 8 pg/mL, respectively.

[b] The signals of the particles detecting the target-present cases are averaged.

[c] The recovery rate was calculated by dividing the measured concentration by the actual spiked-in concentration.

Table S3. Clinical sample analysis with multiplex detection of IL-4, IL-5, IL-6, IL-9, and IL-17 using hydrogel MP-based TSA assay with SH-PEG.

Clinical sample	*Assay method*	*Control Subtracted Signal [a] (a.u.)*				
		IL-4	***IL-5***	***IL-6***	***IL-9***	***IL-17***
Sample A	**Without TSA**	95.9 ± 17.2	102.4 ± 10.8	115.2 ± 13.2	24.4 ± 2.8	8.9 ± 9.6
	TSA assay with SH-PEG	4974.1 ± 755.5	34956.2 ± 1474.6	8597.5 ± 182.0	1174.8 ± 108.9	29648.4 ± 1472.6
Sample B	**Without TSA**	3.1 ± 2.9	1.9 ±3.0	1.6 ± 0.04	2.4 ± 2.1	1.9 ± 1.5
	TSA assay with SH-PEG	31.2 ± 4.7	935.4 ± 150.4	309.0 ± 24.9	190.3 ± 14.5	609.0 ± 67.1

[a] All signals subtracted the control signal (signals of case 1) to exclude the non-specific signals. Each signal is expressed as the mean ± standard deviation of >7 particles.

References

1. Xie, Huancheng, et al. "Pseudomonas aeruginosa exotoxin A as a novel allergen induced Non-TH2 inflammation in a murine model of steroid-insensitive asthma." *Heliyon* 10.18 (2024).

2. An, Ran, et al. "Effect of Epstein–Barr virus on macrophage M2/M1 migration and EphA2 expression in adverse drug reactions." *The Journal of Dermatology* 52.1 (2025): 87-96.